Accepted Manuscript

Minimized natural versions of fungal ribotoxins show improved active site plasticity

Moisés Maestro-López, Miriam Olombrada, Lucía García-Ortega, Daniel Serrano-González, Javier Lacadena, Mercedes Oñaderra, José G. Gavilanes, Álvaro Martínez-del-Pozo

PII: S0003-9861(17)30034-6

DOI: 10.1016/j.abb.2017.03.002

Reference: YABBI 7446

To appear in: *Archives of Biochemistry and Biophysics*

Received Date: 18 January 2017

Revised Date: 3 March 2017

Accepted Date: 5 March 2017

Please cite this article as: M. Maestro-López, M. Olombrada, L. García-Ortega, D. Serrano-González, J. Lacadena, M. Oñaderra, J.G. Gavilanes, E. Martínez-del-Pozo, Minimized natural versions of fungal ribotoxins show improved active site plasticity, *Archives of Biochemistry and Biophysics* (2017), doi: 10.1016/j.abb.2017.03.002.

Minimized natural versions of fungal ribotoxins show improved active site plasticity

Moisés Maestro-López[‡], Miriam Olombrada[†], Lucía García-Ortega, Daniel Serrano-González, Javier Lacadena, Mercedes Oñaderra, José G. Gavilanes and Álvaro Martínez-del-Pozo*

Departamento de Bioquímica y Biología Molecular I, Facultad de Ciencias Químicas, Universidad Complutense, 28040 Madrid, Spain.

[†]Present address: Department of Evolutionary Biology and Environmental Studies, University of Zurich, Winterthurerstrasse 190, 8057 Zurich, Switzerland.

[‡]Present address: Departamento de Estructura de Macromoléculas, Centro Nacional de Biotecnología (CNB-CSIC), Darwin 3, 28049 Madrid, Spain

*Corresponding author: Tel: 34 91 394 4259; E.mail: alvaromp@quim.ucm.es

Abstract

Fungal ribotoxins are highly specific extracellular RNases which cleave a single phosphodiester bond at the ribosomal sarcin-ricin loop, inhibiting protein biosynthesis by interfering with elongation factors. Most ribotoxins show high degree of conservation, with similar sizes and amino acid sequence identities above 85%. Only two exceptions are known: Hirsutellin A and anisoplin, produced by the entomopathogenic fungi *Hirsutella thompsonii* and *Metarhizium anisopliae*, respectively. Both proteins are similar but smaller than the other known ribotoxins (130 vs 150 amino acids), displaying only about 25% sequence identity with them. They can be considered minimized natural versions of their larger counterparts, best represented by α-sarcin. The conserved α-sarcin active site residue Tyr48 has been replaced by the geometrically equivalent Asp, present in the minimized ribotoxins, to produce and characterize the corresponding mutant. As a control, the inverse anisoplin mutant (D43Y) has been also studied. The results show how the smaller versions of ribotoxins represent an optimum compromise among conformational freedom, stability, specificity, and active-site plasticity which allow these toxic proteins to accommodate the characteristic abilities of ribotoxins into a shorter amino acid sequence and more stable structure of intermediate size between that of other nontoxic fungal RNases and previously known larger ribotoxins

Keywords: RNases; insecticidal; sarcin; hirsutellin; anisoplin

Abbreviations: CD, circular dichroism; HtA, Hirsutellin A; PDB, Protein Data Bank; SEM, standard error of the mean; SRL, sarcin-ricin loop; WT, wild-type, T_m, melting temperature.

Fungal ribotoxins are a unique group of highly specific extracellular RNases [1, 2] initially discovered as antitumoral agents [3]. The toxicity of these ribotoxins relies on their ability to cleave a singular phosphodiester bond strategically located at a universally conserved sequence of the large rRNA [4], known as the sarcin-ricin loop (SRL). Therefore, ribosomes are their natural substrates. Cleavage of this single bond inhibits protein biosynthesis, interfering with the function of elongation factors [5-7] and leading to cell death by apoptosis [8]. Given the universal conservation of the SRL sequence, all known ribosomes are susceptible to ribotoxins action. However, these toxic RNases show different affinity against ribosomes from different origins and, above all, they first have to cross the plasmatic membrane to be able to cleave their substrate and exert their cytotoxic activity [9-11]. This behavior explains why not all cells are equally targeted by these toxins. Intriguingly, they are especially active on transformed or virus-infected cells [3, 8, 12] due to an altered permeability of their membrane in combination with an enrichment in acidic phospholipids [8, 11, 13-15]. This feature has been lately related to the possibility of ribotoxins acting as natural insecticidal agents [16-18].

α-Sarcin, restrictocin, Aspf1, and hirsutellin A (HtA) are the most exhaustively characterized ribotoxins [10, 11, 19-26], but many others have been identified and partially characterized in different fungal species [27-35]. Most of them show a high degree of conservation, with similar sizes and amino acid sequence identities above 85% [1, 18, 33]. So far only two exceptions are known: HtA [23, 24, 32] and the recently discovered anisoplin [35], produced by the entomopathogenic fungi *Hirsutella thompsonii* and *Metarhizium anisopliae*, respectively. Both proteins are highly similar but smaller than the other known ribotoxins (130 residues vs 150), displaying only about 25% sequence identity with them [23, 24, 32, 35]. Therefore, they can be considered as minimized natural versions of their larger counterparts. This lower sequence identity and size do not however preclude the conservation of the elements of ordered secondary structure as well as the identity and geometric arrangement of the residues configuring the active site (Figure 1). This structural conservation can be even extended to the other non-toxic members of the larger fungal extracellular RNases family, such as RNase T1 and RNase U2, for example [36, 37]. In fact, comparison of all these RNases three-dimensional structures reveals the strict conservation of the active site residues forming their catalytic triad, His50, Glu96, and His137 in α-sarcin [38], for example, as well as the preservation of a highly hydrophobic residue at the position corresponding to α-sarcin's Leu145 [39] (Figure 1). On the other hand, the presence of an Asp residue in HtA [40] and anisoplin [35] in a position equivalent to α-sarcin Tyr48 [41] must be highlighted as a novelty in the active site of this family of toxic RNases (Figure 1). This is a quite intriguing observation in the context that substitution of this Tyr48 by Phe rendered a α-sarcin variant which was catalytically incompetent, unable to inactivate the ribosome [41]. Interestingly, studies with HtA mutants D40N and D40N/E66Q demonstrated an important role for Asp40 in the activity of

HtA in establishing a new set of electrostatic interactions different from the one described for the already known larger ribotoxins [40].

In the work herein presented α-sarcin Tyr 48 has been replaced by an Asp residue to produce and characterize the corresponding Y48D mutant. As a control, the corresponding inverse anisoplin mutant (D43Y) has been also studied. The results shown reveal the key role of these residues not only in maintaining the correct electrostatic environment and active site plasticity in each type of ribotoxins but also in the preservation of their characteristic high thermostability.

MATERIALS AND METHODS

Mutant cDNA construction

All materials and reagents were of molecular biology grade. Cloning procedures, PCR-based oligonucleotide site-directed mutagenesis, and bacterial manipulations were carried out as previously described [11, 16, 41-43]. Mutagenesis constructions were performed using different sets of complementary mutagenic primers (Table S1). Mutations were confirmed by DNA sequencing at the corresponding Complutense University facility. The plasmids used as templates for mutagenesis, containing the cDNA sequence of either wild-type α-sarcin or anisoplin, have already been described [35, 38, 42].

Protein production and purification

Escherichia coli RB791 or BL21 (DE3) cells, the latter ones being previously cotransformed with a thioredoxin-producing plasmid (pT-Trx), and the corresponding wild-type or mutant plasmids were used to produce and purify all proteins from the periplasmic soluble fraction, as previously described [35, 38, 42, 44-46]. The only exception was fungal wild-type α-sarcin which was isolated from *Aspergillus giganteus* MDH18894, its natural source, following the procedure reported before [11]. SDS-PAGE of proteins, Western blots, protein hydrolysis, and amino acid analysis were performed according to standard procedures, also as previously described [11, 42]. All four proteins studied were purified to homogeneity according to their SDS-PAGE behavior and amino acid analysis.

Spectroscopic characterization

Spectroscopic characterization was performed following well established procedures [11, 22, 38, 41, 44, 47-51]. Absorbance measurements were carried out on a Shimadzu UV-1800 at 200 nm/min scanning speed and room temperature. Amino acid analyses and the corresponding UV absorbance spectra were also used to calculate their extinction coefficients (Table 1). Circular dichroism (CD) spectra were obtained in a Jasco 715 spectropolarimeter (Jasco, Easton, MD, USA), equipped with a thermostated cell holder and a Neslab-111 circulating water bath, at 50 nm/min scanning speed. Thermal denaturation profiles were recorded by measuring the temperature dependence of the

ellipticity at 220 nm in the 25 – 80ºC range using a rate of temperature increment of 30ºC per hour. Fluorescence emission spectra were recorded on an SLM Aminco 8000 spectrofluorimeter at 25ºC using a slit width of 4 nm for both excitation and emission beams. The spectra were recorded for excitation at 275 and 295 nm and both were normalized by considering that Tyr emission above 380 nm is negligible. The Tyr contribution was calculated as the difference between the two normalized spectra. Thermostated cells with a path length of 0.2 and 1.0 cm for the excitation and emission beams, respectively, were used. All these experiments were performed in 50 mM sodium phosphate, pH 7.0.

Ribonucleolytic activity assays

The ribonucleolytic activity of ribotoxins on rabbit ribosomes was followed by detecting the release of a specific 400-nt rRNA fragment, known as the α-fragment, from the ribosomes of a cell-free rabbit reticulocyte lysate (Promega) as described [7, 21, 43, 52]. Visualization of this α-fragment was performed by ethidium bromide staining of 2.0% agarose gels after electrophoretic fractionation of the samples using denaturing conditions. The protein concentration needed to produce 50% of cleavage of the 28S rRNA (IC_{50} value) was determined to evaluate proteins' specific ribonucleolytic activity.

The specific cleavage by ribotoxins of a 35-mer synthetic oligonucleotide mimicking the sequence and structure of the SRL was also analyzed as described before [7, 43, 53]. The sequence of this oligo was 5'-GGGAAUCCUGCUCAGUACGAGAGGAACCGCAGGUU -3', where the cleavage site by α-sarcin appears underlined. Synthesis of this SRL-like RNA oligo was performed as previously described [7, 21]. Reaction products were run on a denaturing 19% (w/v) polyacrylamide gel and visualized by ethidium bromide staining.

RESULTS

Spectroscopic characterization

Far-UV CD spectra of wild-type α-sarcin and the corresponding Y48D mutant showed some differences but were still similar enough as to consider that both proteins displayed a practically identical overall globular fold (Figure 2). Analysis using different software or online tools has been proven to be not very useful in the particular case of ribotoxins given their small size, their high degree of β-sheet content and, above all, the highly unusual contribution of aromatic side-chains within this wavelength range [50, 54-56]. However, the observed differences can be explained by minor local changes attributable to the proximity of Trp51, an amino acid residue showing a non-negligible contribution in the far-UV wavelength region due to its involvement in a cation-π interaction with the ring of His82 (Figure 3) [43, 50]. This interaction would be disturbed in the Y48D mutant. In agreement with this hypothesis, Trp emission (Figure 4) was also shown to be more

heterogeneous, blue-shifted, and four-fold enhanced in the Y48D mutant (Table 1), as expected from an increased hydrophobic microenvironment around the side-chain of Trp51, upon disappearance of the mentioned cation-π interaction. In accordance with this observation, and with the reported existence of tyrosine to Trp51 non-radiative energy transfer in the wild-type protein [50], Tyr emission was also two-fold higher in the Y48D mutant (Figure 4, Table 1), in spite of being a protein species with one Tyr residue less.

A similar situation took place when examining the far-UV CD features of wild-type anisoplin and its D43Y variant; however differences were larger (Figure 2). The spectrum of the wild-type protein corresponds to a protein with a high content of β-sheet, non-ordered structures and aromatic amino acid residues [26, 35, 55, 57], and the observed changes can be attributed to the local contribution of the introduction of the new Tyr residue within the active site of the protein (Figure 2). A global conformational change cannot be however dismissed. Analysis of the fluorescence emission of wild-type anisoplin upon excitation at 275 nm revealed the existence of a contribution centered at 320 nm (Figure 5) which should not be attributable to Tyr residues because they barely emit around this wavelength. This emission would rather be an indication of the already reported different microenvironment surrounding anisoplin Trp residues [35]. This emission disappears in the D43Y mutant, together with the appearance of a 4 nm red-shift of the Trp spectra (from 333 to 337 nm, Figure 5). This set of results, including the far-UV CD spectra, is therefore consistent with a relaxation of anisoplin conformational global fold which exposes Trp side-chains to a less apolar environment. On the other hand Tyr emission remains practically undetectable in spite of the introduction of a new Tyr residue in this mutant.

Thermostability of both mutants

All four proteins studied showed thermograms compatible with the existence of a well-defined two-state thermal transition, confirming the adoption of a folded conformation (Figure S1). Both wild-type α-sarcin and anisoplin are thermostable proteins with T_m values of 52 [48, 54] and 61ºC [16], respectively (Table 1). Introduction of the Asp residue within the α-sarcin active-site resulted in a dramatic reduction of the T_m value to 39ºC (Table 1). Accordingly, the production yield of this mutant increased 15-fold when the *E. coli* cells harboring the corresponding plasmid were grown at 25ºC instead of the standard temperature of 37ºC (Table 1). This argument does not however justify the low yield obtained for wild-type anisoplin (Table 1) which is not easy to explain given the present knowledge in the ribotoxins' field. It can be speculated that, in comparison to α-sarcin, wild-type anisoplin would be more effective against prokaryotic than mammalian ribosomes. This feature would be probably lost in the D43Y mutant after the introduction of the Tyr residue within its active site (Table 1). Interestingly, this reverse mutation in anisoplin introduced a dramatic stabilization of the protein, with a Tm value 14ºC higher than the wild-type protein (Table 1). In agreement with this observation, the fluorescence

emission spectra of this mutant in the presence or the absence of 6 M urea were practically indistinguishable (Figure 7) suggesting that the protein is still folded in the presence of high concentrations of this denaturing agent.

Functional characterization

Ribotoxins are highly specific RNases against intact ribosomes, and they retain this specificity when assayed against naked rRNA containing the SRL [1, 11, 21]. Therefore, two different types of specific enzymatic assays are usually performed to measure their enzymatic activity. The first, and most specific, is one that uses ribosomes within a rabbit cell-free reticulocyte lysate [21]. Their highly specific cleavage can be then visualized by detecting the release of a 400-nucleotide long rRNA fragment (the α-fragment) on a denaturing agarose gel stained with ethidium bromide. The second assay frequently used is based on the employment of short oligoribonucleotides mimicking the SRL sequence and structure. Ribotoxins cleave specifically these SRL-like oligos, producing only two smaller fragments which can be fractionated on a polyacrylamide gel [21, 58]. This cleavage is still specific but several orders of magnitude less efficient than that produced on intact ribosomes because it lacks important recognition determinants which are present at the intact full ribosomes [20, 48, 49, 59-61].

As thoroughly described before [1, 38, 42, 44, 51], wild-type α-sarcin was fully competent against rabbit ribosomes showing an IC_{50} value of about 80 nM (Fig. 6). On the other hand, α-sarcin Y48D was completely inactive by both criteria (Figure 6). This observation is in agreement with previous studies where the removal of the hydroxyl group in the phenol ring of Tyr48 rendered a catalytically inactive protein [41]. Tyr48 appears to be an essential residue of α-sarcin's active site. On the other hand, wild-type anisoplin showed less activity than α-sarcin when assayed against intact ribosomes (IC_{50} = 930 nM), as described before [35], whereas the D43Y mutant was at least as active (IC_{50} = 440 nM) as its wild-type counterpart (Figure 7). However, this mutant also remained completely inactive when assayed against the SRL-like oligomer (Figure 7), a substrate which lacks many of the recognition regions needed for the specific catalytic action of ribotoxins.

DISCUSSION

The ribotoxins family has been thoroughly characterized over the past decades, focused especially in α-sarcin and restrictocin, which are structurally very similar to non-toxic ribonucleases (Figure 1). The discovery of smaller versions of these toxins, like HtA and anisoplin, has prompted a change in the idea that all ribotoxins share a highly similar structure. These "minimized" versions show identical specificity towards their substrate, the SRL at the ribosome, but they share little amino-acid identity and have lost some structural arrangements when compared to "canonical" ribotoxins like α-sarcin. In order to understand these changes and how they may affect the functionality of ribotoxins, we have

produced different variants of α-sarcin and anisoplin where a key residue has been interchanged. Particularly, Tyr48 in α-sarcin, which is essential for the catalytic activity of α-sarcin [41] has been substituted for Asp, present in the smaller ribotoxins HtA and anisoplin. Moreover, anisoplin Asp 3 has been also replaced for Tyr, to mimic α-sarcin Tyr48. According to previous data, the native conformation of α-sarcin is preserved upon conservative changes like the Y48F mutation [41]. In this new study the changes introduced are more dramatic, involving charge changes that most likely will disturb the local electrostatic arrangement, which is critical for the activity of the proteins studied [62-64].

It has been reported how substitution of α-sarcin Trp51 by Phe results in pronounced changes in the far-UV CD spectrum of the protein [50], highly resembling the spectrum obtained now for the Y48D mutant (Figure 2A). This is explained because α-sarcin Trp51 displays a non-negligible contribution in the far-UV wavelength region due to its involvement in a cation-π interaction with the ring of His82 (Figure 3) [43, 50]. As a consequence of this interaction, Trp51 fluorescence emission is also practically undetectable in the wild-type protein [50]. The far-UV CD spectrum of the Y48D α-sarcin mutant suggests that this interaction is disturbed. In agreement with this hypothesis, Trp emission was more heterogeneous (Figure 4) and four-fold enhanced in the Y48D mutant (Table 1), suggesting that the disappearance of the cation-π interaction would increase the hydrophobicity of the microenvironment around the side-chain of Trp51. This interpretation agrees with a very similar observation, reported before, for another mutant where His82 was the residue replaced (by Gln) making impossible the establishment of the mentioned cation-π interaction [43]. Therefore, the far-UV CD small differences and Trp emission changes observed can be explained by the local perturbation produced by the removal of an aromatic moiety (Tyr48) in the spatial proximity of Trp51 (Figure 3) together with the introduction of an additional negative charge.

The spectroscopic characterization of α-sarcin Y48D also revealed a 2-fold increase in the Tyr emission (Figure 4, Table 1). In the wild-type protein, Tyr48 fluorescence emission is completely quenched, and there is a Tyr to Trp51 non-radiative energy transfer [41, 50]. By substituting Tyr for Asp the local configuration of Trp51 is altered, impeding the energy transfer and therefore, increasing the fluorescence emission.

Detailed analysis of the spectroscopic features of the other mutant protein studied, anisoplin D43Y, leads to different conclusions. First of all, the fluorescence emission of the 5 Tyr residues is barely detected, even in the wild-type protein (Figure 5). This emission still goes undetected after the mutation, even though the change performed introduces a new Tyr residue. On the other hand, the Trp population becomes more homogeneous and solvent-exposed, at least in terms of their fluorescence emission behavior, as shown by the red-shift in the spectrum (Figure 5). The far-UV CD changes observed (Figure 2) also point towards this direction. The small size of the protein, altogether with its high content in β-sheet structure and non-ordered loops, results in a spectrum which is highly susceptible to

changes in the environment of its quite abundant Trp residues (Table 1). Overall, the results obtained from the spectroscopic characterization of anisoplin D43Y suggest the induction of local changes within the active site of the protein, as shown for the α-sarcin mutant, but also a relaxation of the global protein fold which results in the mentioned homogenization of the Trp residues microenvironment.

Replacement of Tyr48 by the negatively charged side-chain of an Asp residue seems to strongly destabilize α-sarcin. In α-sarcin, Glu140 displays unusual backbone torsional angles forming a salt bridge with Lys11 in the N-terminal β-hairpin (Figure 8) [63]. This interaction, together with a well-defined network of hydrogen bonds, helps to maintain the orientation of loop 5 [38, 51] and defines the required optimum hydrophobic environment for enzymatic activity. Furthermore, His50, another key residue for activity [38], also appears in the spatial vicinity of the mutated residue (Figure 3), whereas the network of interactions involving Tyr106, Lys114 and Y48 is also essential for catalysis (Figure 8) [43]. These interactions would be disrupted in the Y48D mutant. It appears that the presence of an aromatic residue (Y48) within the active center would be critical for maintaining the local interactions that render a high thermostable and specific RNase. This idea is supported by the functional studies, which show that the α-sarcin Y48D mutant completely loses its activity against rRNA specific substrates, such as ribosomes or a SRL-like oligomer (Figure 6).

A very different picture emerges, however, when a minimized ribotoxin such as anisoplin is studied. Replacement of Asp43 by Tyr yielded an extremely heat resistant variant (Table 1), which agrees with the loss of thermostability of α-sarcin Y48D mutant. This extremely resistant protein did not display any ribonucleolytic activity when assayed against the specific naked rRNA represented by the SRL-like substrate (Figure 7). This Asp 43 residue must be very important in an additional set of interactions that only appears in minimized ribotoxins, just as suggested before for HtA while characterizing different mutations of this Asp (D40N, D40N/E66Q) [40]. On the other hand, the now studied anisoplin D43Y mutant was fully active when assayed against intact ribosomes, suggesting that the conservation of not yet determined interactions other than those ones involved in the specific recognition of the SRL sequence seem to be extremely important for substrate recognition. This set of results further supports the proposal that the active site of these minimized ribotoxins such as anisoplin or HtA would show a higher degree of plasticity than their known larger counterparts [16], being able to accommodate electrostatic and structural changes not suitable for the other previously characterized larger ribotoxins.

Ribotoxins are considered natural engineered proteins evolved from the non-toxic ribonucleases [65]. The newly characterized "minimized" ribotoxins, like HtA or anisoplin, represent a compromise among conformational freedom, stability, specificity and active site plasticity that allows these proteins to accommodate the characteristic abilities of ribotoxins into a shorter amino acid sequence. These smaller versions of ribotoxins may present new

and yet unexplored structural arrangements, being our study one of the first in this direction.

Acknowledgements

This work was supported by project AE1/16-20695 from the Universidad Complutense (Madrid, Spain). M.Ol. was recipient of a FPU predoctoral fellowship from the Spanish Ministerio de Educación. L.G.-O. was a postdoctoral researcher of the PICATA program from the Campus de Excelencia Internacional Moncloa.

Author contributions

MML, MOl, LGO, and DSG designed and performed the experiments and analyzed the data. JL, MOñ, JGG and AMP designed and supervised the research and discussed the data. All authors wrote the manuscript and approved its final version.

References

1. Lacadena, J., Álvarez-García, E., Carreras-Sangrà, N., Herrero-Galán, E., Alegre-Cebollada, J., García-Ortega, L., Oñaderra, M., Gavilanes, J. G. & Martínez-del-Pozo, A. (2007) Fungal ribotoxins: molecular dissection of a family of natural killers, *FEMS Microbiol Rev.* **31**, 212-237.
2. Olombrada, M., Lázaro-Gorines, R., López-Rodríguez, J. C., Martínez-del-Pozo, A., Oñaderra, M., Maestro-López, M., Lacadena, J., Gavilanes, J. G. & García-Ortega, L. (2017) Fungal Ribotoxins: A Review of Potential Biotechnological Applications, *Toxins.* **9**, 71.
3. Jennings, J. C., Olson, B. H., Roga, V., Junek, A. J. & Schuurmans, D. M. (1965) α-Sarcin, a New Antitumor Agent. II. Fermentation and Antitumor Spectrum, *Appl Microbiol.* **13**, 322-326.
4. Schindler, D. G. & Davies, J. E. (1977) Specific cleavage of ribosomal RNA caused by α-sarcin, *Nucleic Acids Res.* **4**, 1097-1110.
5. Nierhaus, K. H., Schilling-Bartetzko, S. & Twardowski, T. (1992) The two main states of the elongating ribosome and the role of the α-sarcin stem-loop structure of 23S RNA, *Biochimie.* **74**, 403-10.
6. Brigotti, M., Rambelli, F., Zamboni, M., Montanaro, L. & Sperti, S. (1989) Effect of α-sarcin and ribosome-inactivating proteins on the interaction of elongation factors with ribosomes, *Biochem J.* **257**, 723-7.
7. García-Ortega, L., Álvarez-García, E., Gavilanes, J. G., Martínez-del-Pozo, A. & Joseph, S. (2010) Cleavage of the sarcin-ricin loop of 23S rRNA differentially affects EF-G and EF-Tu binding, *Nucleic Acids Res.* **38**, 4108-19.
8. Olmo, N., Turnay, J., González de Buitrago, G., López de Silanes, I., Gavilanes, J. G. & Lizarbe, M. A. (2001) Cytotoxic mechanism of the ribotoxin α-sarcin. Induction of cell death via apoptosis, *Eur J Biochem.* **268**, 2113-2123.
9. Oñaderra, M., Mancheño, J. M., Gasset, M., Lacadena, J., Schiavo, G., Martínez-del-Pozo, A. & Gavilanes, J. G. (1993) Translocation of α-sarcin across the lipid bilayer of asolectin vesicles, *Biochem J.* **295**, 221-225.

10. Gasset, M., Mancheño, J. M., Lacadena, J., Turnay, J., Olmo, N., Lizarbe, M. A., Martínez-del-Pozo, A., Oñaderra, M. & Gavilanes, J. G. (1994) α-Sarcin, a ribosome-inactivating protein that translocates across the membrane of phospholipid vesicles, *Curr Top Pept Protein Res.* **1**, 99-104.
11. Martínez-Ruiz, A., García-Ortega, L., Kao, R., Lacadena, J., Oñaderra, M., Mancheño, J. M., Davies, J., Martínez-del-Pozo, A. & Gavilanes, J. G. (2001) RNase U2 and α-sarcin: A study of relationships, *Methods Enzymol.* **341**, 335-351.
12. Fernández-Puentes, C. & Carrasco, L. (1980) Viral infection permeabilizes mammalian cells to protein toxins, *Cell.* **20**, 769-75.
13. Gasset, M., Oñaderra, M., Thomas, P. G. & Gavilanes, J. G. (1990) Fusion of phospholipid vesicles produced by the anti-tumour protein α-sarcin, *Biochem J.* **265**, 815-22.
14. Gasset, M., Martínez-del-Pozo, A., Oñaderra, M. & Gavilanes, J. G. (1989) Study of the interaction between the antitumour protein α-sarcin and phospholipid vesicles, *Biochem J.* **258**, 569-75.
15. Masip, M., Lacadena, J., Mancheño, J. M., Oñaderra, M., Martínez-Ruiz, A., Martínez-del-Pozo, A. & Gavilanes, J. G. (2001) Arginine 121 is a crucial residue for the specific cytotoxic activity of the ribotoxin α-sarcin, *Eur J Biochem.* **268**, 6190-6196.
16. Olombrada, M., Garía-Ortega, L., Lacadena, J., Oñaderra, M., Gavilanes, J. G. & Martínez-Del-Pozo, A. (2016) Involvement of loop 5 lysine residues and the N-terminal β-hairpin of the ribotoxin hirsutellin A on its insecticidal activity, *Biol Chem.* **397**, 135-45.
17. Olombrada, M., Herrero-Galán, E., Tello, D., Oñaderra, M., Gavilanes, J. G., Martínez-del-Pozo, A. & García-Ortega, L. (2013) Fungal extracellular ribotoxins as insecticidal agents, *Insect Biochem Mol Biol.* **43**, 39-46.
18. Olombrada, M., Martínez-del-Pozo, A., Medina, P., Budia, F., Gavilanes, J. G. & García-Ortega, L. (2014) Fungal ribotoxins: Natural protein-based weapons against insects, *Toxicon.* **83**, 69-74.
19. Arruda, L. K., Mann, B. J. & Chapman, M. D. (1992) Selective expression of a major allergen and cytotoxin, Asp f I, in *Aspergillus fumigatus*. Implications for the immunopathogenesis of Aspergillus-related diseases, *J Immunol.* **149**, 3354-9.
20. Wool, I. G. (1997) Structure and mechanism of action of the cytotoxic ribonuclease α-sarcin in *Ribonucleases* (D'Alessio, G. & Riordan, J. F., eds) pp. 131-162, Academic Press Inc, San Diego.
21. Kao, R., Martínez-Ruiz, A., Martínez-del-Pozo, A., Crameri, R. & Davies, J. (2001) Mitogillin and related fungal ribotoxins, *Methods Enzymol.* **341**, 324-335.
22. García-Ortega, L., Lacadena, J., Villalba, M., Rodríguez, R., Crespo, J. F., Rodríguez, J., Pascual, C., Olmo, N., Oñaderra, M., Martínez-del-Pozo, A. & Gavilanes, J. G. (2005) Production and characterization of a noncytotoxic deletion variant of the *Aspergillus fumigatus* allergen Asp f 1 displaying reduced IgE binding, *FEBS J.* **272**, 2536-44.
23. Boucias, D. G., Farmerie, W. G. & Pendland, J. C. (1998) Cloning and sequencing of cDNA of the insecticidal toxin hirsutellin A, *J Invertebr Pathol.* **72**, 258-61.
24. Herrero-Galán, E., Lacadena, J., Martínez-del-Pozo, A., Boucias, D. G., Olmo, N., Oñaderra, M. & Gavilanes, J. G. (2008) The insecticidal protein hirsutellin A from the mite fungal pathogen *Hirsutella thompsonii* is a ribotoxin, *Proteins.* **72**, 217-228.
25. Maimala, S., Tartar, A., Boucias, D. & Chandrapatya, A. (2002) Detection of the toxin Hirsutellin A from *Hirsutella thompsonii*, *J Invertebr Pathol.* **80**, 112-26.

26. Viegas, A., Herrero-Galán, E., Oñaderra, M., Macedo, A. L. & Bruix, M. (2009) Solution structure of hirsutellin A. New insights into the active site and interacting interfaces of ribotoxins, *FEBS J.* **276**, 2381-2390.
27. Lin, A., Huang, K. C., Hwu, L. & Tzean, S. S. (1995) Production of type II ribotoxins by *Aspergillus* species and related fungi in Taiwan, *Toxicon.* **33**, 105-110.
28. Parente, D., Raucci, G., Celano, B., Pacilli, A., Zanoni, L., Canevari, S., Adobati, E., Colnaghi, M. L., Dosio, F., Arpicco, S., Cattel, L., Mele, A. & De Santis, R. (1996) Clavin a type-1 ribosome-inactivating protein from *Aspergillus clavatus* IFO 8605 - cDNA isolation, heterologous expression, biochemical and biological characterization of the recombinant protein, *Eur J Biochem.* **239**, 272-280.
29. Huang, K.-C., Hwang, Y.-Y., Hwang, L. & Lin, A. (1997) Characterization of a new ribotoxin gene (c-sar) from *Aspergillus clavatus*, *Toxicon.* **35**, 383-392.
30. Wirth, J., Martínez-del-Pozo, A., Mancheño, J. M., Martinez-Ruiz, A., Lacadena, J., Oñaderra, M. & Gavilanes, J. G. (1997) Sequence determination and molecular characterization of gigantin, a cytotoxic protein produced by the mould *Aspergillus giganteus* IFO 5818, *Arch Biochem Biophys.* **343**, 188-193.
31. Martínez-Ruiz, A., Kao, R., Davies, J. & Martínez-del-Pozo, A. (1999) Ribotoxins are a more widespread group of proteins within the filamentous fungi than previously believed, *Toxicon.* **37**, 1549-1563.
32. Martínez-Ruiz, A., Martínez-del-Pozo, A., Lacadena, J., Oñaderra, M. & Gavilanes, J. G. (1999) Hirsutellin A displays significant homology to microbial extracellular ribonucleases, *J Invertebr Pathol.* **74**, 96-97.
33. Herrero-Galán, E., García-Ortega, L., Olombrada, M., Lacadena, J., Martínez-del-Pozo, A., Gavilanes, J. G. & Oñaderra, M. (2013) Hirsutellin A: A Paradigmatic Example of the Insecticidal Function of Fungal Ribotoxins, *Insects.* **4**, 339-356.
34. Varga, J. & Samson, R. A. (2008) Ribotoxin genes in isolates of *Aspergillus* section *Clavati*, *Antonie Van Leeuwenhoek.* **94**, 481-485.
35. Olombrada, M., Medina, P., Budia, F., Gavilanes, J. G., Martínez-Del-Pozo, A. & García-Ortega, L. (2017) Characterization of a new toxin from the entomopathogenic fungus *Metarhizium anisopliae*: the ribotoxin anisoplin, *Biol Chem.* **398**, 135-142.
36. Pace, C. N., Heinemann, U., Hahn, U. & Saenger, W. (1991) Ribonuclease T1: Structure, function and stability, *Angew Chem Int Ed Engl.* **30**, 343-360.
37. Noguchi, S., Satow, Y., Uchida, T., Sasaki, C. & Matsuzaki, T. (1995) Crystal structure of Ustilago sphaerogena ribonuclease U2 at 1.8 angstrom resolution, *Biochemistry.* **34**, 15583-15591.
38. Lacadena, J., Martínez-del-Pozo, A., Martínez-Ruiz, A., Pérez-Cañadillas, J. M., Bruix, M., Mancheño, J. M., Oñaderra, M. & Gavilanes, J. G. (1999) Role of histidine-50, glutamic acid-96, and histidine-137 in the ribonucleolytic mechanism of the ribotoxin α-sarcin, *Proteins.* **37**, 474-484.
39. Masip, M., García-Ortega, L., Olmo, N., García-Mayoral, M. F., Pérez-Cañadillas, J. M., Bruix, M., Oñaderra, M., Martínez-del-Pozo, A. & Gavilanes, J. G. (2003) Leucine 145 of the ribotoxin α-sarcin plays a key role for determining the specificity of the ribosome-inactivating activity of the protein, *Prot Science.* **12**, 161-169.
40. Herrero-Galán, E., García-Ortega, L., Lacadena, J., Martínez-Del-Pozo, A., Olmo, N., Gavilanes, J. G. & Oñaderra, M. (2012) Implication of an Asp residue in the

ribonucleolytic activity of hirsutellin A reveals new electrostatic interactions at the active site of ribotoxins, *Biochimie.* **94**, 427-433.
41. Álvarez-García, E., García-Ortega, L., Verdun, Y., Bruix, M., Martínez-del-Pozo, A. & Gavilanes, J. G. (2006) Tyr-48, a conserved residue in ribotoxins, is involved in the RNA-degrading activity of α-sarcin, *Biol Chem.* **387**, 535-41.
42. Lacadena, J., Martínez-del-Pozo, A., Barbero, J. L., Mancheño, J. M., Gasset, M., Oñaderra, M., López-Otín, C., Ortega, S., García, J. L. & Gavilanes, J. G. (1994) Overproduction and purification of biologically active native fungal α-sarcin in *Escherichia coli*, *Gene.* **142**, 147-151.
43. Castaño-Rodríguez, C., Olombrada, M., Partida-Hanon, A., Lacadena, J., Oñaderra, M., Gavilanes, J. G., García-Ortega, L. & Martínez-del-Pozo, A. (2015) Involvement of loops 2 and 3 of α-sarcin on its ribotoxic activity, *Toxicon.* **96**, 1-9.
44. García-Ortega, L., Lacadena, J., Lacadena, V., Masip, M., de Antonio, C., Martínez-Ruiz, A. & Martínez-del-Pozo, A. (2000) The solubility of the ribotoxin α-sarcin, produced as a recombinant protein in *Escherichia coli*, is increased in the presence of thioredoxin, *Lett Appl Microbiol.* **30**, 298-302.
45. Mancheño, J. M., Gasset, M., Albar, J. P., Lacadena, J., Martinez-del-Pozo, A., Oñaderra, M. & Gavilanes, J. G. (1995) Membrane interaction of a β-structure-forming synthetic peptide comprising the 116-139th sequence region of the cytotoxic protein α-sarcin, *Biophys J.* **68**, 2387-95.
46. Siemer, A., Masip, M., Carreras, N., García-Ortega, L., Oñaderra, M., Bruix, M., Martínez del Pozo, A. & Gavilanes, J. G. (2004) Conserved asparagine residue 54 of α-sarcin plays a role in protein stability and enzyme activity, *Biol Chem.* **385**, 1165-70.
47. Álvarez-García, E., Martínez-del-Pozo, A. & Gavilanes, J. G. (2009) Role of the basic character of α-sarcin's NH_2-terminal β-hairpin in ribosome recognition and phospholipid interaction, *Arch Biochem Biophys.* **481**, 37-44.
48. García-Ortega, L., Lacadena, J., Mancheño, J. M., Oñaderra, M., Kao, R., Davies, J., Olmo, N., Martínez-del-Pozo, A. & Gavilanes, J. G. (2001) Involvement of the amino-terminal β-hairpin of the *Aspergillus* ribotoxins on the interaction with membranes and nonspecific ribonuclease activity, *Protein Sci.* **10**, 1658-68.
49. García-Ortega, L., Masip, M., Mancheño, J. M., Oñaderra, M., Lizarbe, M. A., García-Mayoral, M. F., Bruix, M., Martínez-del-Pozo, A. & Gavilanes, J. G. (2002) Deletion of the NH_2-terminal β-hairpin of the ribotoxin α-sarcin produces a nontoxic but active ribonuclease, *J Biol Chem.* **277**, 18632-9.
50. De Antonio, C., Martínez-del-Pozo, A., Mancheño, J. M., Oñaderra, M., Lacadena, J., Martínez-Ruiz, A., Pérez-Cañadillas, J. M., Bruix, M. & Gavilanes, J. G. (2000) Assignment of the contribution of the tryptophan residues to the spectroscopic and functional properties of the ribotoxin α-sarcin, *Proteins.* **41**, 350-61.
51. Lacadena, J., Mancheño, J. M., Martínez-Ruiz, A., Martínez-del-Pozo, A., Gasset, M., Oñaderra, M. & Gavilanes, J. G. (1995) Substitution of histidine-137 by glutamine abolishes the catalytic activity of the ribosome-inactivating protein α-sarcin, *Biochem J.* **309**, 581-586.
52. Herrero-Galán, E., García-Ortega, L., Lacadena, J., Martínez-Del-Pozo, A., Olmo, N., Gavilanes, J. G. & Oñaderra, M. (2012) A non-cytotoxic but ribonucleolytically specific ribotoxin variant: implication of tryptophan residues in the cytotoxicity of hirsutellin A, *Biol Chem.* **393**, 449-456.

53. Olombrada, M., Rodríguez-Mateos, M., Prieto, D., Pla, J., Remacha, M., Martínez-del-Pozo, A., Gavilanes, J. G., Ballesta, J. P. & García-Ortega, L. (2014) The acidic ribosomal stalk proteins are not required for the highly specific inactivation exerted by α-sarcin of the eukaryotic ribosome, *Biochemistry.* **53**, 1545-1547.
54. Martínez-del-Pozo, A., Gasset, M., Oñaderra, M. & Gavilanes, J. G. (1988) Conformational study of the antitumor protein α-sarcin, *Biochim Biophys Acta.* **953**, 280-288.
55. Lacadena, J., Martínez-del-Pozo, A., Gasset, M., Patiño, B., Campos-Olivas, R., Vázquez, C., Martínez-Ruiz, A., Mancheño, J. M., Oñaderra, M. & Gavilanes, J. G. (1995) Characterization of the antifungal protein secreted by the mould *Aspergillus giganteus*, *Arch Biochem Biophys.* **324**, 273-81.
56. Woody, R. W. a. D., A.K. (1996) Aromatica and cysteine side-chain CD in proteins, *Circular dichroism and Conformational Analysis of Biomolecules*, *109-175*.
57. Woody, R. W. (1978) Aromatic side-chain contributions to the far ultraviolet circular dichroism of peptides and proteins, *Biopolymers.* **17**, 1451-1467.
58. Endo, Y., Chan, Y.-L., Lin, A., Tsurugi, K. & Wool, I. (1988) The cytotoxins α-sarcin and ricin retain their specificity when tested on a synthetic oligoribonucleotide (35-mer) that mimics a region of 28 S ribosomal ribonucleic acid., *J Biol Chem.* **263**, 7917-7920.
59. Glück, A. & Wool, I. G. (1996) Determination of the 28 S ribosomal RNA identity element (G4319) for α-sarcin and the relationship of recognition to the selection of the catalytic site, *Journal of Molecular Biology.* **256**, 838-848.
60. García-Mayoral, F., García-Ortega, L., Álvarez-García, E., Bruix, M., Gavilanes, J. G. & Martínez-del-Pozo, A. (2005) Modeling the highly specific ribotoxin recognition of ribosomes, *FEBS Lett.* **579**, 6859-64.
61. García-Mayoral, M. F., García-Ortega, L., Lillo, M. P., Santoro, J., Martínez-del-Pozo, A., Gavilanes, J. G., Rico, M. & Bruix, M. (2004) NMR structure of the noncytotoxic α-sarcin mutant Δ(7-22): the importance of the native conformation of peripheral loops for activity, *Protein Sci.* **13**, 1000-1011.
62. Pérez-Cañadillas, J. M., Campos-Olivas, R., Lacadena, J., Martínez-del-Pozo, A., Gavilanes, J. G., Santoro, J., Rico, M. & Bruix, M. (1998) Characterization of pKa values and titration shifts in the cytotoxic ribonuclease α-sarcin by NMR. Relationship between electrostatic interactions, structure, and catalytic function, *Biochemistry.* **37**, 15865-15876.
63. Pérez-Cañadillas, J. M., Santoro, J., Campos-Olivas, R., Lacadena, J., Martínez-del-Pozo, A., Gavilanes, J. G., Rico, M. & Bruix, M. (2000) The highly refined solution structure of the cytotoxic ribonuclease α-sarcin reveals the structural requirements for substrate recognition and ribonucleolytic activity, *J Mol Biol.* **299**, 1061-1073.
64. Campos-Olivas, R., Bruix, M., Santoro, J., Martínez-del-Pozo, A., Lacadena, J., Gavilanes, J. G. & Rico, M. (1996) Structural basis for the catalytic mechanism and substrate specificity of the ribonuclease α-sarcin, *FEBS Lett.* **399**, 163-165.
65. Kao, R. & Davies, J. (1999) Molecular dissection of mitogillin reveals that the fungal ribotoxins are a family of natural genetically engineered ribonucleases, *J Biol Chem.* **274**, 12576-12582.
66. Martinez-Oyanedel, J., Choe, H. W., Heinemann, U. & Saenger, W. (1991) Ribonuclease T1 with free recognition and catalytic site: crystal structure analysis at 1.5 A resolution, *J Mol Biol.* **222**, 335-52.

522 67. Noguchi, S. (2010) Structural changes induced by the deamidation and isomerization
523 of asparagine revealed by the crystal structure of *Ustilago sphaerogena* ribonuclease U2B,
524 *Biopolymers.* **93**, 1003-10.
525 68. Noguchi, S. (2010) Isomerization mechanism of aspartate to isoaspartate implied by
526 structures of *Ustilago sphaerogena* ribonuclease U2 complexed with adenosine 3'-
527 monophosphate, *Acta Crystallogr D Biol Crystallogr.* **66**, 843-9.
528 69. DeLano, W. L. (2008) The PyMOL Molecular Graphics System, *San Diego,*
529 *California*.

530

Table 1. Purification yield, expressed as milligrams of protein isolated per one liter of original culture grown at 37ºC, and spectroscopic parameters of the wild-type and mutant proteins studied. Relative fluorescence emission yields (Q_{Trp} and Q_{Tyr}) are referred to the values of the wild-type proteins. T_m values are also shown.

Protein	**Purification yield[a)]**	**$E^{0.1\%}$ b)**	**Number of Tyr**	**Number of Trp**	**Q_{Trp}**	**Q_{Tyr}**	**T_m (ºC)**
α-Sarcin WT	7.0	1.34	8	2	1.00	1.00	52
α-Sarcin Y48D	0.1[c)]	1.24	7	2	4.08	2.35	39
Anisoplin WT	0.5	1.62	5	3	1.00	-	61
Anisoplin D43Y	6.2	1.44	6	3	0.92	-	75

a) Expressed as mg per liter of original bacterial culture.

[b)] $E^{0.1\%}$ (280 nm, 1.0 cm).

[c)] This yield increased to 1.5 mg when cells were grown at 25ºC in accordance with the highly diminished T_m value of this mutant.

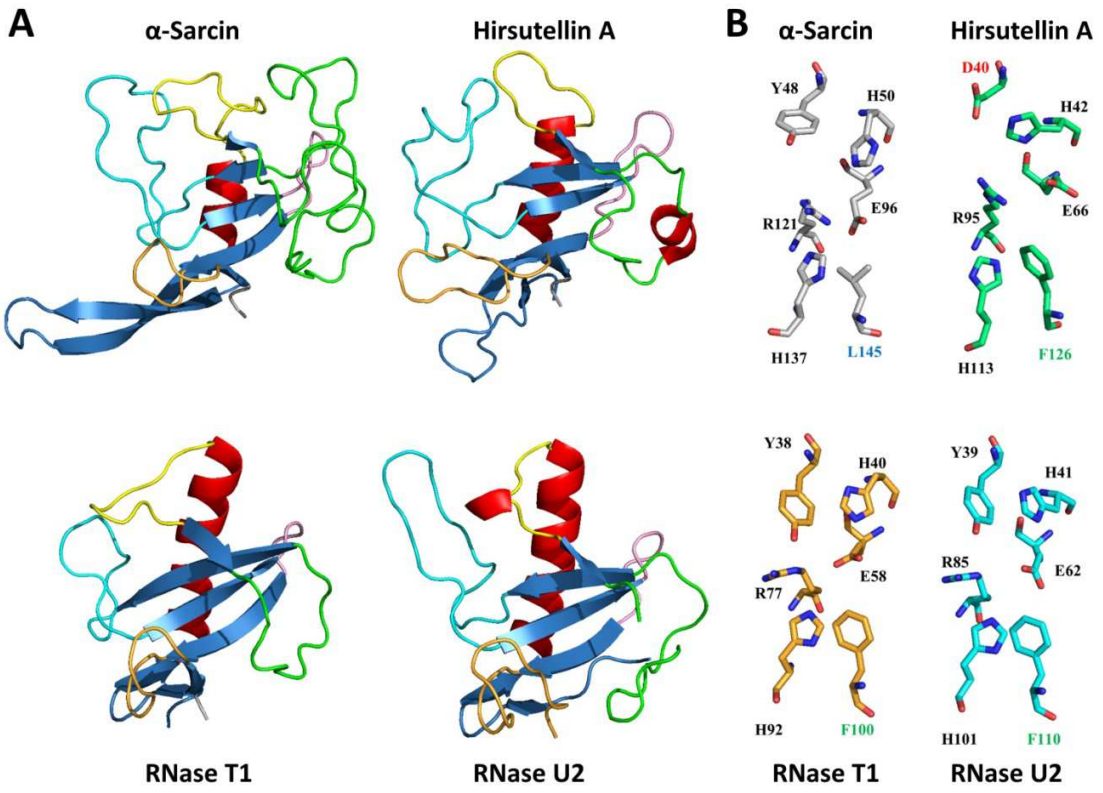

Figure 1: Representation of the three-dimensional structure and active center geometric arrangement of representative fungal RNases. (A) Diagrams showing the three-dimensional structure of ribotoxins α-sarcin (PDB ID: 1DE3) [63] and HtA (PDB ID: 2KAA) [26], and two non-toxic fungal extracellular RNases from the same family: RNases T1 (9RNT) [36, 66] and U2 (1RTU) [37, 67, 68]. (B) Geometric arrangement of the active site residues of these same four RNases. The catalytic triad made of two His and one Glu residues is conserved in all proteins shown while a fourth residue, the equivalent to α-sarcin Leu145, maintains its highly hydrophobic character (Phe or Leu). The position corresponding to α-sarcin Tyr48 is also conserved except for HtA and anisoplin (not shown) where the equivalent position is occupied by an Asp residue (D40, in red). Diagrams were generated using the PyMol software [69].

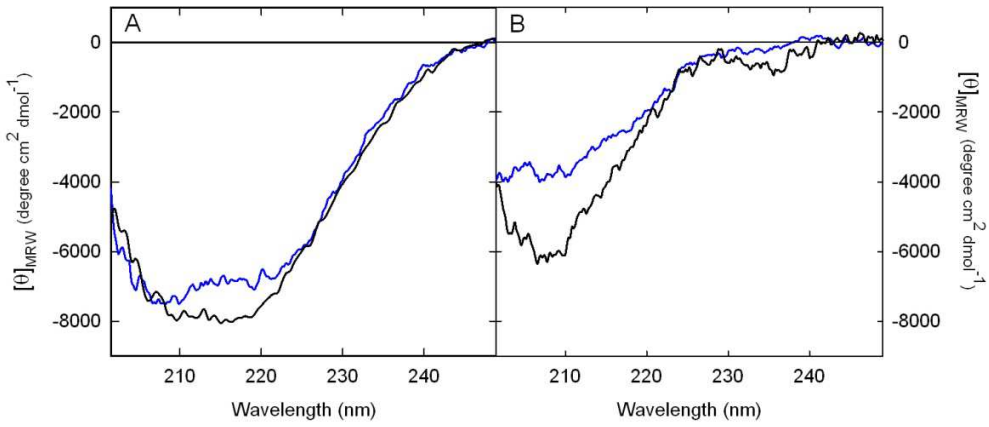

553

554 **Figure 2. Far-UV CD spectra of the ribotoxins studied**. Wild-type α-sarcin (A) and
555 anisoplin (B) ribotoxins (black lines) and their corresponding Y48D (A) and D43Y (B)
556 mutant variants (blue lines). Results are shown as mean residue weight ellipticity ($[\theta]_{MRW}$)
557 values expressed in units of degree x cm^2 x $dmol^{-1}$.

558

559 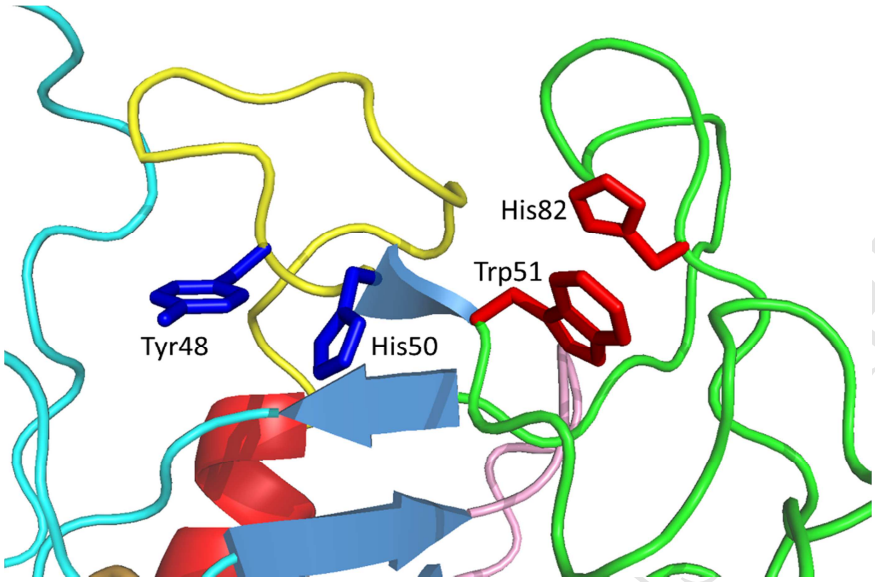

560 **Figure 3. Diagram showing the relative spatial positions of Tyr48, His50, Trp51, and**
561 **His82 residues in α-sarcin**. There is a cation-π interaction between Trp51 and His82 [50,
562 62, 63]. Diagram was generated using the PyMol software [69] and the corresponding PDB
563 coordinates (PDB ID: 1DE3).

564

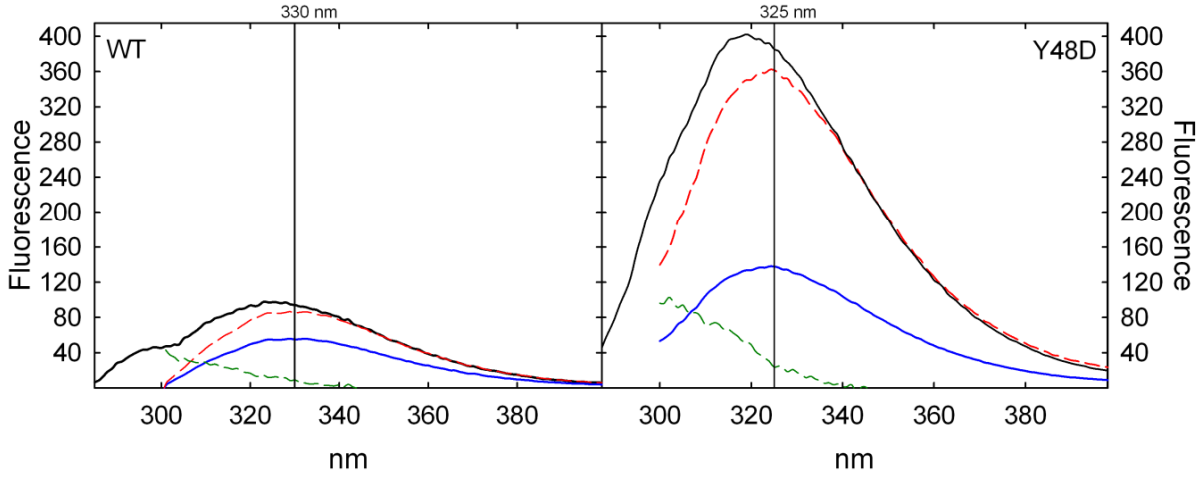

Figure 4. Fluorescence emission spectra of wild-type α-sarcin and its Y48D mutant. All spectra were recorded at identical protein concentrations. Spectra were recorded at excitation wavelengths of 275 nm (continuous black line) and 295 nm (continuous blue line). These two spectra were normalized at wavelengths above 380 nm to obtain the Tryptophan contribution (dashed red line). Tyrosine contribution (dashed green line) was calculated by subtracting the Trp only contribution (dashed red line) from that spectrum obtained after excitation at 275 nm (continuous black line). Fluorescence emission units were arbitrary, and referred to the maximum value of wild-type α-sarcin upon excitation at 275 nm. The positions of the two maxima corresponding to both spectra of the wild-type and Y48D proteins upon excitation at 295 nm are indicated with a vertical black line.

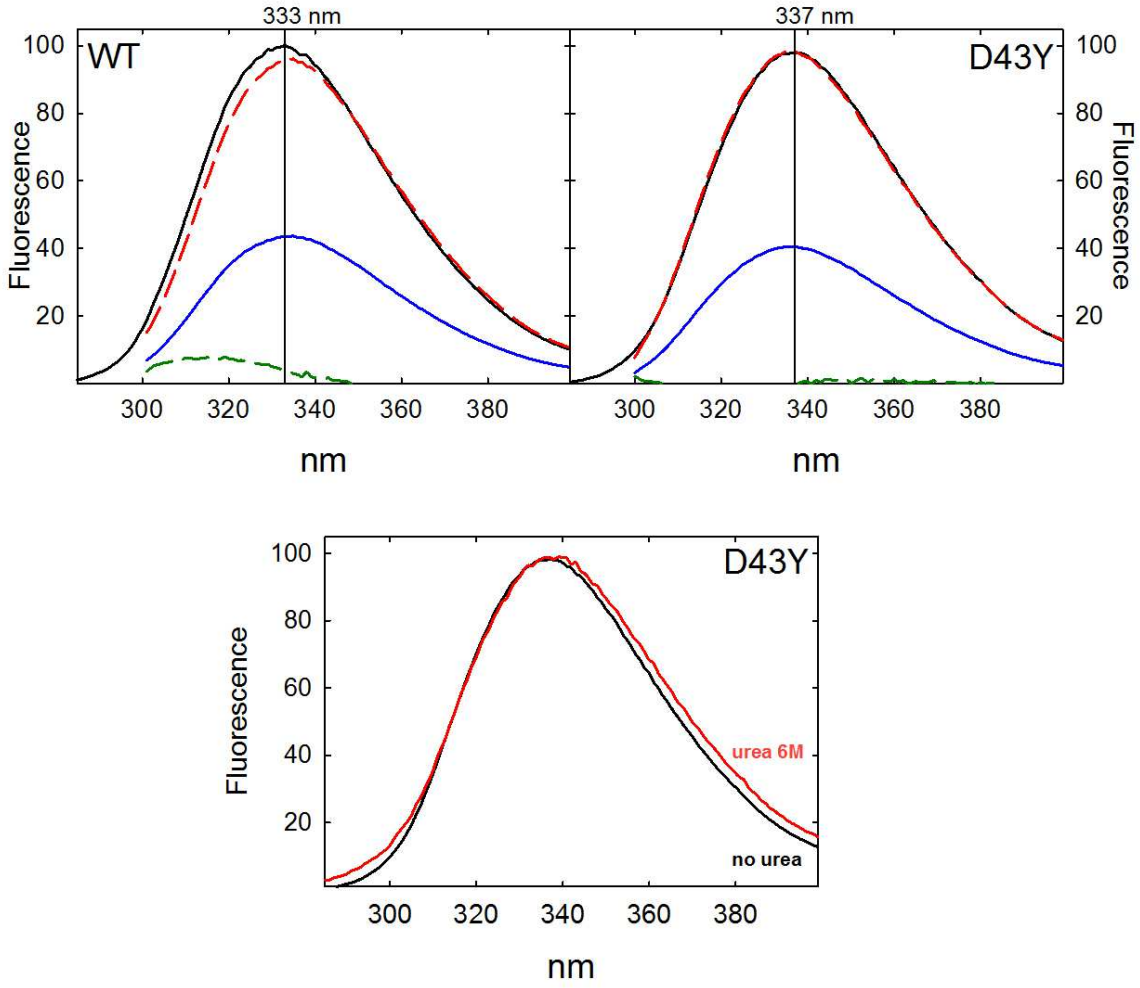

Figure 5. Fluorescence emission spectra of wild-type anisoplin and its D43Y mutant. (*Upper panel*) All spectra were recorded at identical protein concentrations. Spectra were recorded at excitation wavelengths of 275 nm (continuous black line) and 295 nm (continuous blue line). These two spectra were normalized at wavelengths above 380 nm to obtain the Tryptophan contribution (dashed red line). Tyrosine contribution (dashed green line) was calculated by subtracting the Trp only contribution (dashed red line) from that spectrum obtained after excitation at 275 nm (continuous black line). Fluorescence emission units were arbitrary, and referred to the maximum value of wild-type α-sarcin upon excitation at 275 nm. The positions of the two maxima corresponding to both spectra of the wild-type and D43Y proteins upon excitation at 295 nm are indicated with a vertical black line. (*Lower panel*) Fluorescence emission spectra of the anisoplin D43Y mutant, upon excitation at 275 nm, in the absence (black line) or in the presence of 6 M urea (red line).

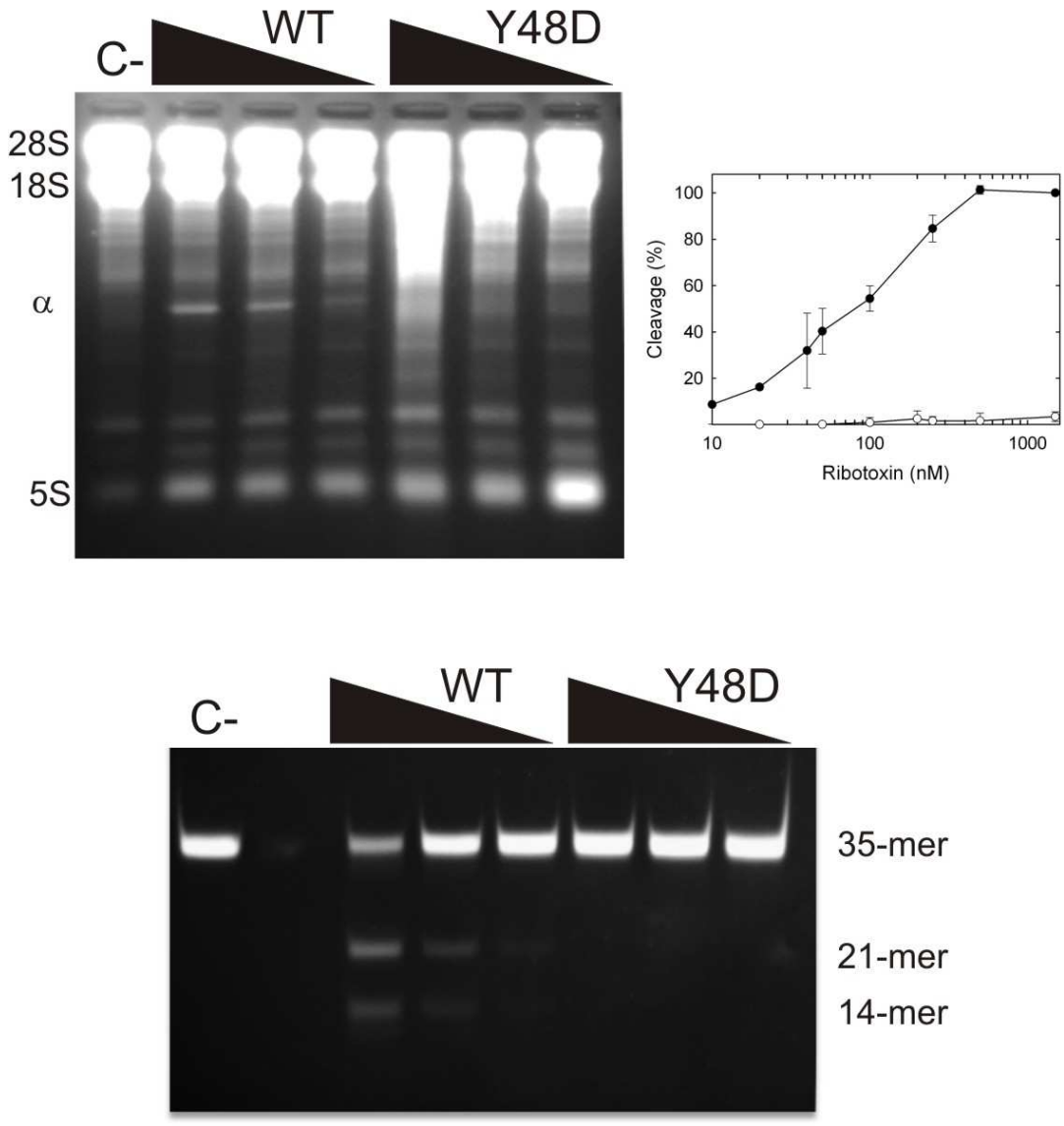

592

593 **Figure 6. Specific ribonucleolytic activity of wild-type α-sarcin and its Y48D mutant.**
594 (*Upper panel*) Ribosome cleaving activity assay performed using a rabbit cell-free
595 reticulocytes lysate. A control in the absence of enzyme is also shown (C-). Protein
596 concentrations shown are 20, 50, and 100 nM. The highly specific ribonucleolytic activity
597 of the ribotoxins is shown by the release of the 400-nt α-fragment (α) from the 28S rRNA
598 of eukaryotic ribosomes. Positions of bands corresponding to 28S, 18S, and 5S rRNA are
599 also indicated. The graph shows the quantitation of two independent experiments with error
600 bars representing ±SEM values. (*Lower panel*) Activity assay on a 35-mer oligonucleotide
601 mimicking the SRL. A control in the absence of enzyme is also shown (C-). Protein
602 concentrations shown are 100, 200, and 500 nM. The 21-mer and 14-mer oligonucleotides
603 resulting from the specific cleavage of a single phosphodiester bond, as well as the intact
604 35-mer oligo are indicated.

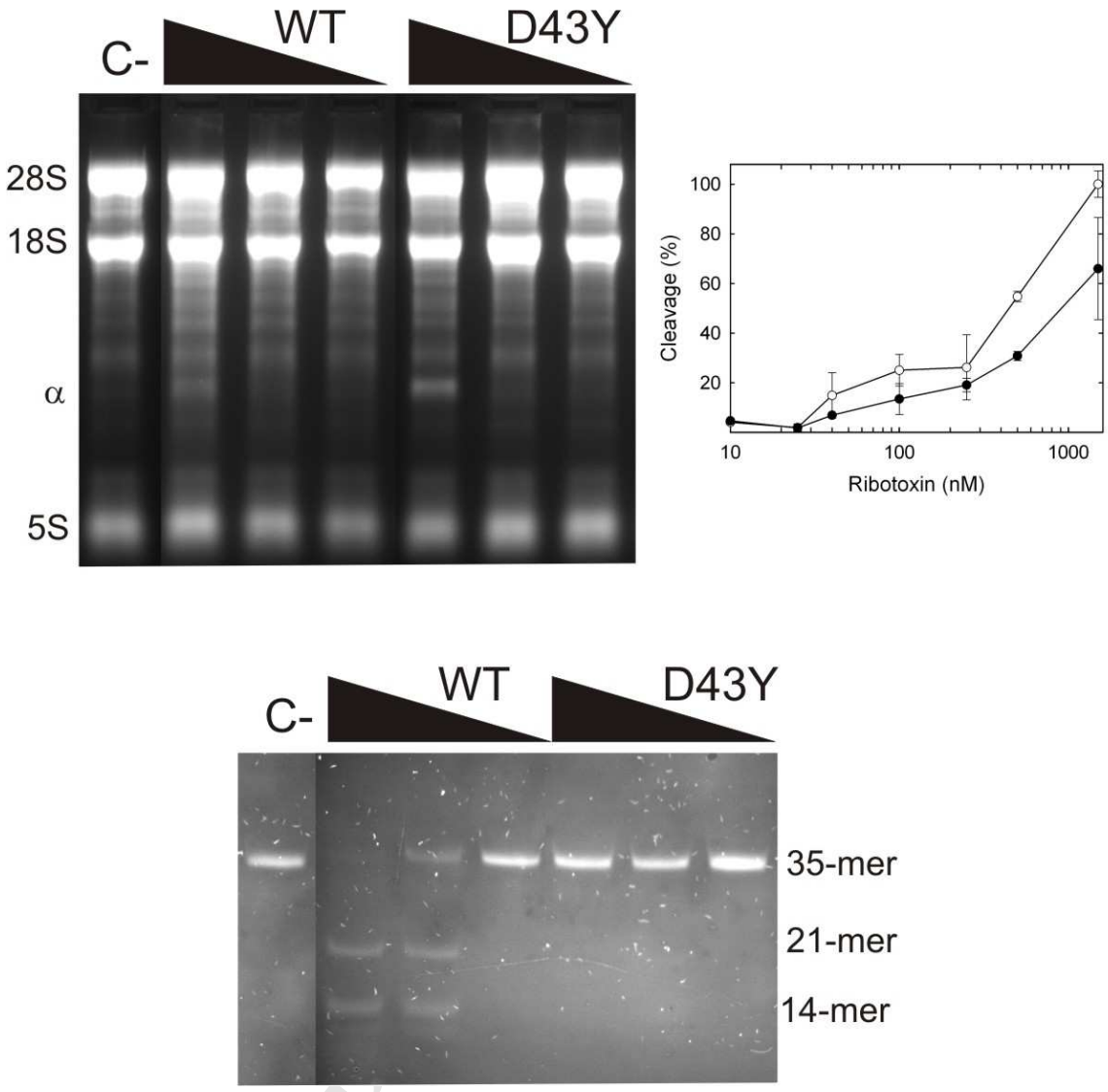

605

606 **Figure 7. Specific ribonucleolytic activity of wild-type anisoplin and its D43Y mutant.**
607 (*Upper panel*) Ribosome cleaving activity assay performed using a rabbit cell-free
608 reticulocytes lysate. A control in the absence of enzyme is also shown (C-). Protein
609 concentrations shown are 2.5, 25, and 250 nM. The highly specific ribonucleolytic activity
610 of the ribotoxins is shown by the release of the 400-nt α-fragment (α) from the 28S rRNA
611 of eukaryotic ribosomes. Positions of bands corresponding to 28S, 18S, and 5S rRNA are
612 also indicated. The graph shows the quantitation of two independent experiments with error
613 bars representing ±SEM values. (*Lower panel*) Activity assay on a 35-mer oligonucleotide
614 mimicking the SRL. A control in the absence of enzyme is also shown (C-). Protein
615 concentrations shown are 10, 50, and 250 nM. The 21-mer and 14-mer oligonucleotides
616 resulting from the specific cleavage of a single phosphodiester bond, as well as the intact
617 35-mer oligo are indicated.

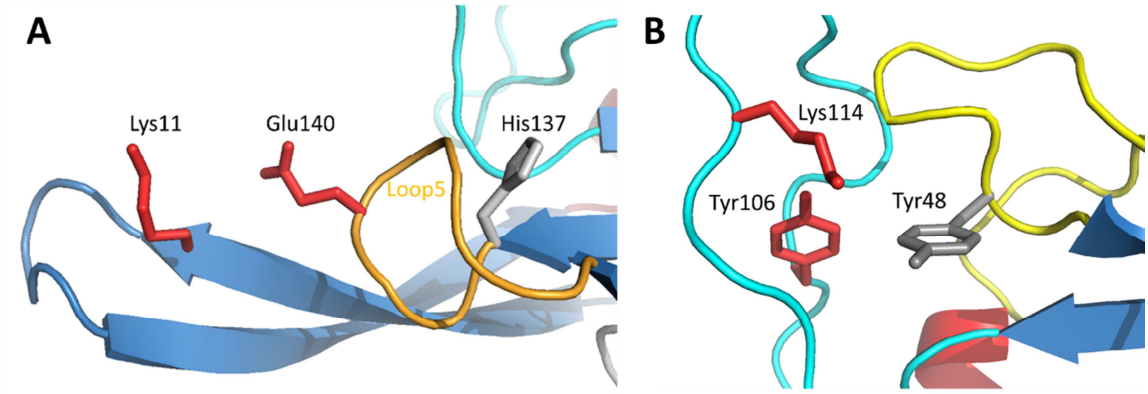

Figure 8. Diagrams showing the relative spatial positions of different amino acid residues in α-sarcin: (A) Lys11, Glu140, and His137; (B) Tyr48, Tyr106 and Lys114. Diagrams were generated using the PyMol software [69] and the corresponding PDB coordinates (PDB ID: 1DE3).